



## OPEN ACCESS

## EDITED BY

Yang Yang,  
Nanjing University of Information Science and  
Technology, China

## REVIEWED BY

Lili Ren,  
Jiangsu Open University, China  
Jiyuan Gao,  
Nanjing University of Information Science and  
Technology, China

## \*CORRESPONDENCE

Gunnar Myhre  
✉ gunnar.myhre@cicero.oslo.no

RECEIVED 07 March 2024

ACCEPTED 21 May 2024

PUBLISHED 12 June 2024

## CITATION

Myhre G, Byrom RE, Andrews T, Forster PM  
and Smith CJ (2024) Efficacy of climate  
forcings in transient CMIP6 simulations.  
*Front. Clim.* 6:1397358.  
doi: 10.3389/fclim.2024.1397358

## COPYRIGHT

© 2024 Myhre, Byrom, Andrews, Forster and  
Smith. This is an open-access article  
distributed under the terms of the [Creative  
Commons Attribution License \(CC BY\)](#). The  
use, distribution or reproduction in other  
forums is permitted, provided the original  
author(s) and the copyright owner(s) are  
credited and that the original publication in  
this journal is cited, in accordance with  
accepted academic practice. No use,  
distribution or reproduction is permitted  
which does not comply with these terms.

# Efficacy of climate forcings in transient CMIP6 simulations

Gunnar Myhre<sup>1\*</sup>, Rachael E. Byrom<sup>1</sup>, Timothy Andrews<sup>2</sup>,  
Piers M. Forster<sup>3</sup> and Christopher J. Smith<sup>3,4</sup>

<sup>1</sup>CICERO Center for International Climate Research, Oslo, Norway, <sup>2</sup>Met Office Hadley Centre, Exeter, United Kingdom, <sup>3</sup>Priestley Centre, University of Leeds, Leeds, United Kingdom, <sup>4</sup>Energy, Climate and Environment Program, International Institute for Applied Systems Analysis, Laxenburg, Austria

For effective radiative forcing (ERF) to be an ideal metric for comparing the strength of different climate drivers (such as CO<sub>2</sub> and aerosols), the ratio of radiative forcing to global-mean temperature change must be the same for each driver. Typically, this ratio is divided by the same ratio for CO<sub>2</sub> and termed efficacy. Previously it has been shown that efficacy is close to unity in abrupt perturbation experiments for a range of climate drivers, but efficacy with respect to CO<sub>2</sub> has not been investigated in transient realistic simulations. Here, we analyse transient simulations from CMIP6 experiments and show comparable results between transient and abrupt perturbation experiments. We demonstrate that aerosol efficacy is not significantly different from unity, however inter-model differences in aerosol experiments are notably large.

## KEYWORDS

effective radiative forcing, imbalance, climate response, climate models, CMIP6

## 1 Introduction

Effective radiative forcing (ERF) has become the preferred metric to quantify the top of atmosphere (TOA) perturbation to the Earth's energy budget by a given climate driver (Boucher et al., 2013; Myhre et al., 2013; Forster et al., 2021). This is because ERF, by definition, includes tropospheric rapid adjustments to the initial perturbation (Hansen et al., 2005; Sherwood et al., 2015) which leads to a more similar equilibrium temperature change for different climate drivers for a given forcing magnitude (Shine et al., 2003; Hansen et al., 2005; Richardson et al., 2019).

The utility of ERF as a metric to compare the relative strength of different climate drivers in inducing surface temperature change is also dependent on the behavior of the climate feedback parameter ( $\alpha$ ; W m<sup>-2</sup> K<sup>-1</sup>), which represents the radiative response of the climate system to temperature change induced by a forcing (Forster et al., 2021). Namely, this dependency relies on whether  $\alpha$  varies with forcing mechanism (Hansen et al., 2005) and time [e.g., Andrews et al. (2015), Rugenstein et al. (2016), Richardson et al. (2019)]. Quantifying the efficacy of different climate drivers (i.e., the global-mean surface temperature response per unit ERF relative to CO<sub>2</sub>) is therefore important for understanding the contribution of various climate drivers throughout the industrial era (Shindell, 2014; Richardson et al., 2019) and for the projection of future temperature trends and climate metrics (Myhre et al., 2013; Forster et al., 2021). The relationship between ERF and temperature change can be described as (Gregory and Andrews, 2016) in Equation (1):

$$dN = dF - \alpha dT \quad (1)$$

where  $dT$  is the global-mean surface temperature change resulting from an ERF ( $dF$ ) from a climate driver and  $dN$  is the TOA energy imbalance. Efficacy (Equation 2) is defined as

Hansen et al. (2005) when the climate system is in equilibrium ( $dN = 0$ ):

$$E = \frac{dT_i/dF_i}{dT_{CO_2}/dF_{CO_2}} \quad (2)$$

where  $dT$  is the global-mean surface temperature change resulting from an ERF ( $F$ ) from climate driver  $i$  (such as non-CO<sub>2</sub> greenhouse gases and aerosols) relative to that for CO<sub>2</sub>. An efficacy of one demonstrates that ERF is ideal for comparing surface temperature changes from different climate drivers, since the magnitude of warming in response to CO<sub>2</sub> forcing is equal to that from  $i$ .

For a climate system not in equilibrium the efficacy becomes as in Equation (3):

$$E = \frac{dT_i/(dF_i - dN_i)}{dT_{CO_2}/(dF_{CO_2} - dN_{CO_2})} \quad (3)$$

Since the climate feedback parameter,  $\alpha = \frac{dF-dN}{dT}$ , efficacy can also be described in terms of the radiative response induced by a forcing, whereby in Equation (4):

$$E = \frac{\alpha_{CO_2}}{\alpha_i} \quad (4)$$

Here an efficacy close to unity illustrates that radiative feedback processes are similar for climate driver  $i$  relative to CO<sub>2</sub>.

Radiative feedbacks act to amplify or dampen climate sensitivity to a forcing and are demonstrated to play an important role in driving different temperature responses for different forcings (Shindell, 2014; Marvel et al., 2016; Smith and Forster, 2021; Salvi et al., 2022). Largely, a forcing occurring in regions with a weaker radiative response results in stronger warming per unit increase in ERF and an efficacy greater than unity. Zhou et al. (2023) calculate the efficacy of 10 different abrupt forcing agents to demonstrate its dependency on a combination of feedback state-dependence (e.g., Ceppi and Gregory (2019)) and “pattern-effect” (Haugstad et al., 2017), whereby different forcings initiate different radiative feedbacks via the pattern of change in sea-surface temperature (SST). They find enhanced warming over tropical regions leads to increased low clouds globally, a weaker lapse rate and more negative TOA radiative fluxes, resulting in a pattern-effect induced efficacy deviating from unity. Further, Zhou et al. (2023) find that a negative change in global surface temperature (e.g., from non-BC aerosol forcing) results in stronger radiative dampening and a reduced efficacy relative to abrupt 2xCO<sub>2</sub> forcing. Comparing aerosols and greenhouse gases (GHGs), Salvi et al. (2022) also consider how historical forcings affect SST and stability and modulate radiative response, concluding that net radiative feedback is stronger for aerosols, consistent with their different latitudinal forcing distribution compared to GHGs; proposing that differences in  $\alpha$  arise from different tropospheric stability responses and the subsequent impact on cloud and lapse-rate feedbacks. To further investigate how the spatial pattern of forcing affects climate feedback and sensitivity, Zhang et al. (2023) perform sensitivity simulations by applying solar forcing over the entire globe, Northern Hemisphere mid-latitudes, Southern

Ocean, and tropics. They show that varied forcing patterns lead to large differences in feedback mechanisms. In particular, the lapse rate feedback and cloud feedback show large regional dependence which is mainly caused by differences in coupling between the surface and troposphere. Overall, their study found that the global mean surface temperature change is doubled when the forcing is imposed over the Southern Ocean compared to when the forcing is applied in the tropics.

Several studies report efficacies that deviate from unity (Hansen et al., 2005; Shindell, 2014; Shindell et al., 2015; Marvel et al., 2016; Modak et al., 2018), largely depending on the model and method used to derive forcing estimates. Richardson et al. (2019) conduct a multi-model analysis of 11 global climate models (GCMs) participating in the Precipitation Driver and Response Model Intercomparison Project [PDRMIP; Myhre et al. (2017)] to diagnose efficacy for abrupt forcing perturbations. With ERF calculated using fixed sea-surface temperatures and sea-ice (fsst) they report a solar forcing (2% increase in insolation) efficacy of less than one across all models (0.77–0.95) with multi-model mean efficacy of slightly less than one for 3x methane (CH<sub>4</sub>; 0.87), 5x sulfate (SO<sub>4</sub>; 0.94) and 10x black carbon (BC; 0.87), with large intermodel spread. They note that multi-model mean efficacy is marginally closer to unity when ERF is adjusted for land-surface temperature change and that efficacy varies substantially for SO<sub>4</sub> and BC model ensembles in particular, causing uncertainty in whether it significantly deviates from unity.

Such abrupt forcing experiments more inherently embody the equilibrium temperature response however, and do not characterize transient changes in ERF,  $\alpha$  and  $dT$ . The novelty in this study is that we analyse CMIP6 transient fully-coupled GCM simulations with ERF diagnosed from corresponding fsst simulations to compare efficacy calculated across the historical period against that diagnosed from abrupt 4xCO<sub>2</sub>.

## 2 Materials and methods

We use results from the CMIP6 DECK simulations (Eyring et al., 2016) and the two CMIP6 MIPs: DAMIP (Gillett et al., 2016) and RFMIP (Pincus et al., 2016). Specifically, we use the DECK fully coupled transient simulations forced by a 1% increase in CO<sub>2</sub> until quadrupling (1pctCO<sub>2</sub>) and by all climate drivers over the industrial era from 1850 to 2014 (historical) along with the DAMIP fully coupled transient simulation of historical change in CO<sub>2</sub> (hist-CO<sub>2</sub>), historical change in all well-mixed greenhouse gases (hist-GHG) and historical change in all aerosols (hist-aer). In addition, we include the fully coupled DECK simulation of abrupt quadrupling of CO<sub>2</sub> (abrupt-4xCO<sub>2</sub>) which is distinct from the aforementioned transient simulations under investigation in this study. This abrupt-4xCO<sub>2</sub> is similar to the setup of all experiments in the PDRMIP study (Richardson et al., 2019).

ERFs are derived from the RFMIP fsst simulations as detailed in Smith et al. (2020) and are calculated relative to the piClim-control reference case following the method denoted as ERF<sub>trop</sub> in Smith et al. (2020), which corrects for land surface change in fsst experiments and the portion of tropospheric temperature and water vapor changes associated with it [also see further discussions in Andrews et al. (2021)]. Tables 1, 2 summarize the models and

TABLE 1 List of models with institutions and resolution.

Model	Institution	Resolution
ACCESS-CM2	Commonwealth Scientific and Industrial Research Organization-Australian Research Council Center of Excellence for Climate System Science	192 × 144
CanESM2	Canadian Center for Climate Modeling and Analysis	128 × 64
CESM2	National Center for Atmospheric Research United States	288 × 192
CNRM-CM6-1	Center National de Recherches Meteorologiques-Center Europeen de Recherche et de Formation Avancee en Calcul Scientifique	256 × 128
CNRM-ESM2-1	Center National de Recherches Meteorologiques-Center Europeen de Recherche et de Formation Avancee en Calcul Scientifique	256 × 128
EC-Earth3-Veg	EC-Earth consortium	512 × 256
GFDL-CM4	National Oceanic and Atmospheric Administration-Geophysical Fluid Dynamics Laboratory	288 × 180
GFDL-ESM4	National Oceanic and Atmospheric Administration-Geophysical Fluid Dynamics Laboratory	288 × 180
GISS-E2-1-G	Goddard Institute for Space Studies	144 × 90
HadGEM3-GC31-LL	Met Office Hadley Center	192 × 144
IPSL-CM6A-LR	Institut Pierre Simon Laplace	144 × 143
MIROC6	Japan Agency for Marine-Earth Science and Technology, Atmosphere and Ocean Research Institute, National Institute for Environmental Studies, and RIKEN Center for Computational Science	256 × 128
MPI-ESM1-2-LR	Max Planck Institute for Meteorology	192 × 96
MRI-ESM2-0	Meteorological Research Institute	320 × 160
NorESM2-LM	NorESM Climate modeling Consortium	144 × 96
NorESM2-MM	NorESM Climate modeling Consortium	288 × 192
UKESM1-0-LL	Met Office Hadley Center	192 × 144

CMIP6 experiments included in this study, respectively. All CMIP6 data used are monthly means.

To calculate efficacy following Equation 3 we use the CMIP6 1pctCO2 experiment until doubling of CO<sub>2</sub> (which occurs at year 70) as the reference CO<sub>2</sub> ERF and surface temperature response for the six other experiments (Table 2), whereby the surface temperature response is calculated as the difference between last 5 years of each fully-coupled experiment and the pre-industrial simulation (piControl). Note, that the 5 years are centered around year 70 in the reference 1pctCO2. To derive an estimate of internal variability, the last 5 years of each experiment are also differenced from 10 different piControl 5-year periods taken from across the simulation length. As given in Equation 3, the TOA imbalance is subtracted from the ERF in each experiment to calculate efficacy

TABLE 2 List of CMIP6 experiments investigated in this study and a description.

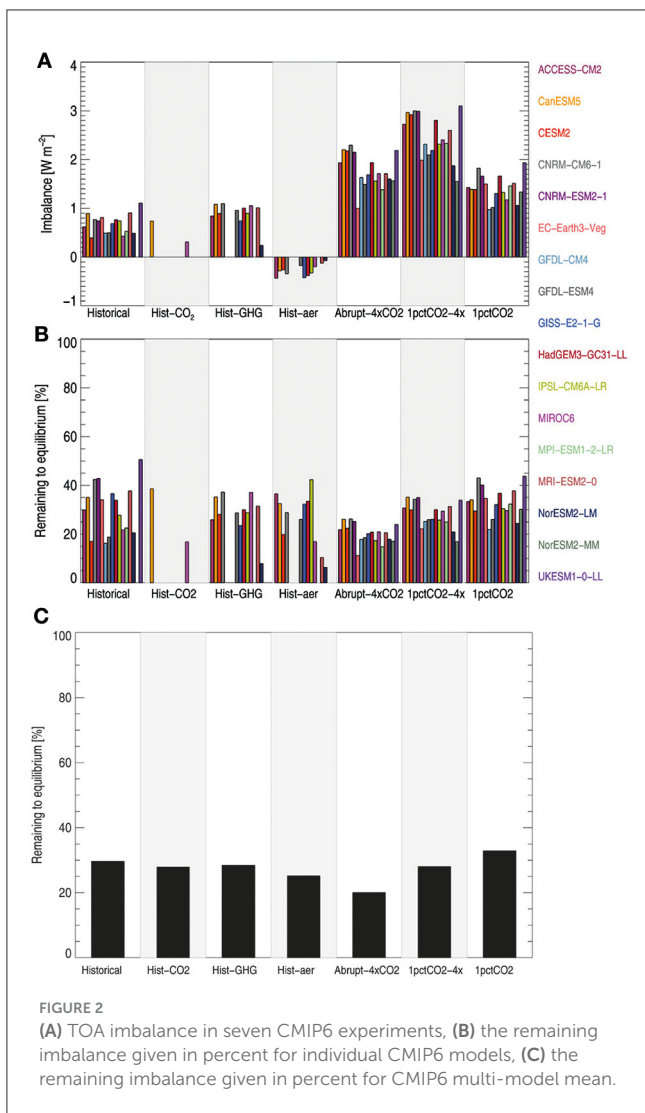
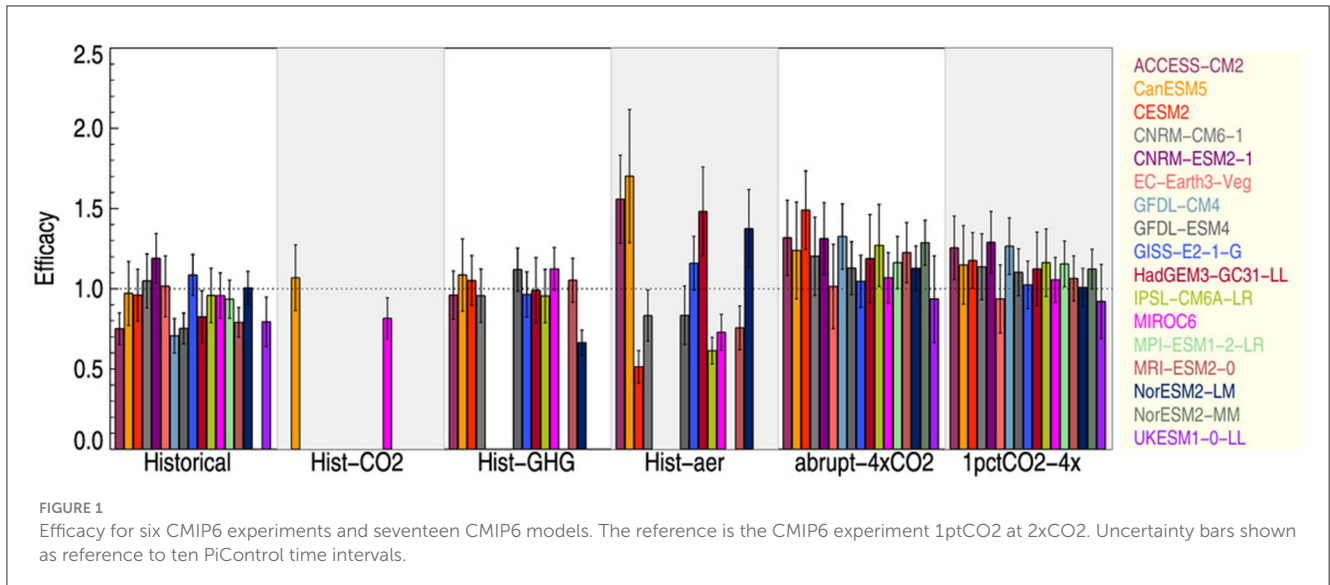
Experiment	Description
historical	Industrial era (1850–2014) simulations with all anthropogenic and natural drivers included.
hist-CO2	Same as Historical, except only the CO <sub>2</sub> forcing included.
hist-GHG	Same as Historical, except only well-mixed greenhouse gases included.
hist-aer	Same as Historical, except only aerosols included.
abrupt-4 × CO2	Abrupt quadrupling of the CO <sub>2</sub> concentration.
1pctCO2	1% yr <sup>-1</sup> CO <sub>2</sub> concentration increase until doubling (occurs after 70 years). The experiment has also been used for 1% yr <sup>-1</sup> CO <sub>2</sub> concentration increase until quadrupling (occurs after 140 years) and denoted here as 1pctCO2-4x.

(Hansen et al., 2005), including the reference 1pctCO2 experiment. Here, the TOA imbalance is calculated as the difference between the given transient CMIP6 experiment listed in Table 2 and the CMIP6 piControl experiment. Note that a line-by-line model (Myhre et al., 2006; Etminan et al., 2016) has been used to establish the relation of doubling of CO<sub>2</sub> to quadrupling of CO<sub>2</sub> since only quadrupling is available from the RFMIP simulations (Smith et al., 2020).

### 3 Results

Figure 1 shows efficacy values for the six CMIP6 experiments, using 1pctCO2 as the reference case. The uncertainty bars represent the outcomes relative to the ten 5-year periods in the piControl simulations. In most models, the hist-GHG experiment has efficacies closest to unity. The hist-GHG experiment includes all major GHGs over the industrial era, with CO<sub>2</sub> being the dominant (Forster et al., 2021). The largest model range in efficacy is in the hist-aer experiment. However, the hist-aer experiment has the weakest ERF and thus the internal variability for the surface temperature response may cause part of the large range in efficacy and large uncertainty range for some of the models. The reasons for the large range in the efficacy in the hist-aer experiment could be manifold, including that models have very different spatial distributions of aerosol, the type of aerosol i.e., absorbing vs. scattering, and their balance between aerosol-radiation interaction and aerosol-cloud interaction (Smith et al., 2020). On top of this the efficacy is dependent on the relation between Northern hemisphere vs. Southern Hemisphere forcing pattern (Zhang et al., 2023), possibly the land vs. ocean forcing (Shindell, 2014) and how the forcing pattern initiates the feedbacks (Haugstad et al., 2017). There is not a clear relation between the results for the historical and hist-aer experiments. All the models have an efficacy above one for the abrupt-4xCO2 experiment, except UKESM1. The efficacy for this experiment is weakly correlated with the effective climate sensitivity (EffCS; 0.35) with EffCS calculated in Zelinka et al. (2020).

Supplementary Figure S1 illustrates the same as Figure 1, except that the TOA imbalance has not been excluded in the calculations of efficacies. In Supplementary Figure S1 unlike in Figure 1, the efficacy is beyond unity for all models in the abrupt-4xCO2 experiment. Of the seven CMIP6 experiments analyzed in this study, the abrupt-4xCO2 and 1pctCO2-4x experiments



have the largest TOA imbalance (Figure 2A). However, these experiments have at least twice as strong an ERF than in the other experiments. Figure 2B shows that the models have responded to about 80% of the initial ERF and thus 20% is remaining to full equilibrium (in abrupt-4xCO<sub>2</sub>). In millennial-length simulations of CO<sub>2</sub> perturbation, the models are close to equilibrating and EffCS is 17% higher than the analysis of the 150 years simulations (Rugenstein et al., 2020). Figures 2B, C shows that the abrupt-4xCO<sub>2</sub> experiment is closer to equilibrium than the other CMIP6 experiments. Among the six other CMIP6 experiments, which are transient simulations, there is a marked similarity in the remaining fraction of imbalance. However, it is apparent that the 1ptCO<sub>2</sub> experiment at 4xCO<sub>2</sub> (year 140) exhibits a relatively smaller imbalance compared to 1ptCO<sub>2</sub> at 2xCO<sub>2</sub>, and likewise with hist-aer contrasted against the historical experiment. The latter effect may be because the rate of increase in negative aerosol forcing has been weaker or has even exhibited a reversal of sign over the last one to two decades of the CMIP6 historical experiments (Smith et al., 2021; Quaas et al., 2022) whilst there has been a continued increase in the GHG forcing (Forster et al., 2021).

Figure 3 shows the geographical distribution of efficacy calculated as the geographical distribution of  $dT_i/dF_i$  divided by the global mean  $\alpha_{CO_2}$ . Note that the imbalance is not taken into account in the figure. Across all experiments, a clear Arctic amplification is evident (Previdi et al., 2021; Rantanen et al., 2022) and efficacies below 1 are common over ocean. The abrupt-4xCO<sub>2</sub> has the highest efficacies (as shown in Figure 1, Supplementary Figure S1) with values around unity over ocean with much higher values over Antarctica than in the other CMIP6 experiments shown here. An interesting feature of the hist-aer experiment is the notably higher efficacies over land in the Northern hemisphere. Moreover, distinct strongly negative local efficacies over the southern hemisphere ocean are evident in the hist-aer experiment relative to the other experiments. The historical and hist-GHG experiments exhibit substantial similarity

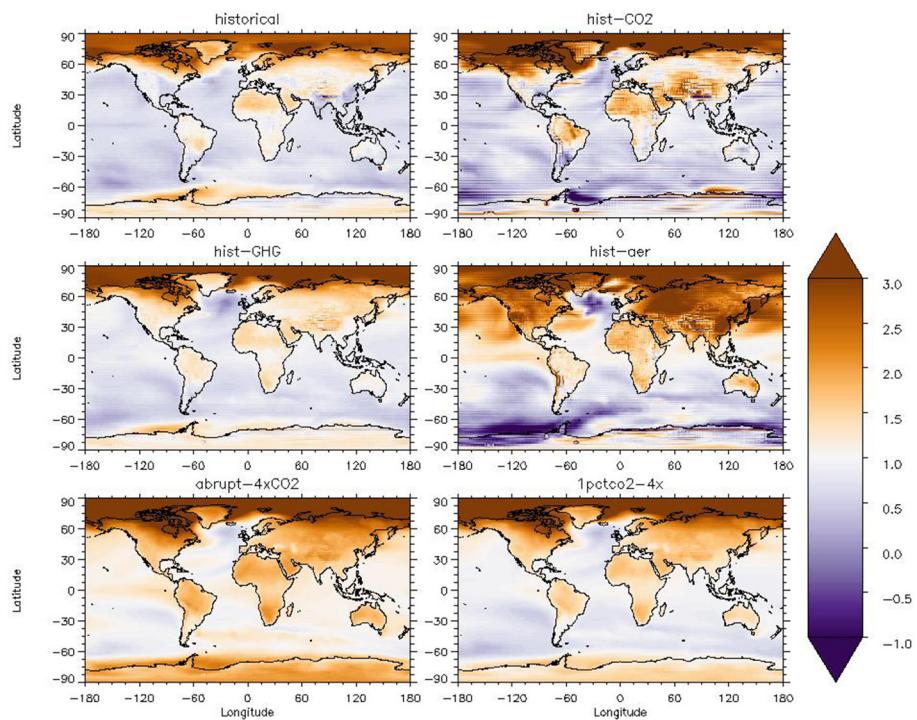


FIGURE 3 Geographical distribution of efficacy for six CMIP6 experiments. Multi-model mean results are shown.

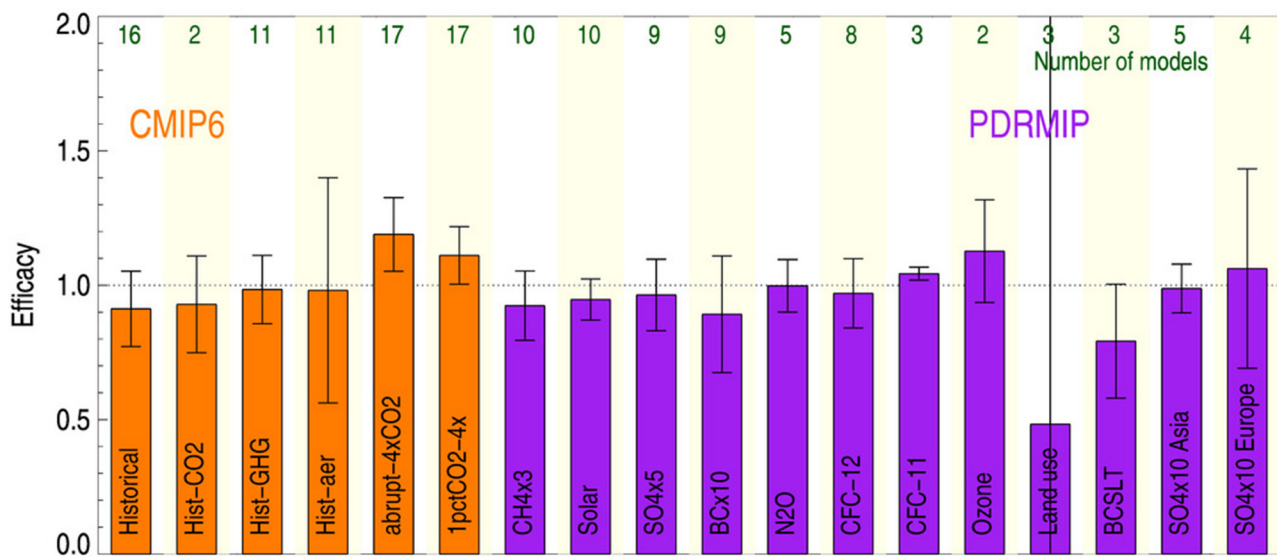


FIGURE 4 Efficacies in CMIP6 and PDRMIP experiments. The bars show the geometric means and uncertainties shown as one standard deviation. The number of model simulations available for each experiment is shown in green.

in most regions. However, deviations arise in areas with elevated anthropogenic aerosol abundance, such as China, India and eastern part of US, where the Historical experiment has efficacies below unity.

Figure 4 shows the geometric mean efficacies from the CMIP6 experiments and compares them to the idealized experiments

within PDRMIP. The PDRMIP results are same as in Richardson et al. (2019), but with the land surface temperature correction incorporated as in Andrews et al. (2021). Overall, the mean efficacies are close to unity, including for the experiments involving aerosols. The finding here is that efficacies in transient experiments are similar to abrupt experiments. Efficacies above unity occur

in experiments with large forcings such as in the quadrupling of CO<sub>2</sub> (transient and abrupt). The largest exception for the unity of efficacy is found for experiments with few models involved such as land use change (land use) and BC specified at lower altitudes in the atmosphere (BCSLT). In both of these experiments the surface temperature response is weak causing the internal variability to play a larger role than in many of the other experiments. In the land use experiment the direct change in the surface fluxes of sensible and latent heat can further cause difference in surface temperature response for a given ERF compared to the other experiments in this study.

## 4 Discussions and conclusions

A main finding from this study is that there is no indication that efficacies for aerosols are very different from unity, as shown in both in the CMIP6 and PDRMIP simulations. However, model differences in the aerosol experiments are much larger than for the other experiments. The advantage of the PDRMIP SO<sub>4</sub>x5 experiment is that a large perturbation is performed, resulting in a robust surface temperature response and thus signal to noise is large. In the other aerosol experiments a low surface temperature response may have contributed to large model deviations in the efficacy.

The spatial pattern of the ERF of anthropogenic aerosol changes for 11 models are shown in [Supplementary Figure S2](#) to investigate further the large range in the efficacy of hist-aer. The magnitude and spatial pattern vary between the models with all models having the strongest negative forcing over South-East Asia. The higher efficacy over land in the Northern hemisphere shown in [Figure 3](#) is not a feature that is causing the hist-aer efficacy to have a large model diversity as shown in [Figure 1](#). The land fraction aerosol ERF is actually slightly anticorrelated ( $-0.25$  Pearson correlation coefficient) to the efficacy for the models in the hist-aer experiment. All models have a stronger aerosol ERF in the tropics relative to the global mean (ratio range from 1.07 to 1.30) and this ratio is moderately anticorrelated ( $-0.58$ ) to the model range in hist-aer efficacy, meaning models with high tropical aerosol ERF generally have low efficacy. The correlation of the efficacy to the fraction of polar aerosol ERF to global mean and fraction of Northern hemisphere to global mean are both low ( $-0.30$  and  $0.24$ , respectively). To draw firm conclusions of temperature response from aerosol perturbations we show that a large model ensemble is required since the model variations are large. We find no systematic cause of this large model diversity in efficacy for aerosol perturbation in terms of aerosol type (sulfate or BC), transient or abrupt or regional aerosol forcing.

Our surface temperature responses have been taken for the 5 last years of transient simulations. Expanding this to 10 years generally changes the efficacy modestly, but somewhat more for the hist-aer experiment (from 0.98 to 1.09 for the geometric mean) than the other experiments. The standard deviation among the models for the hist-aer experiment changes slightly from 0.42 to 0.46 using 10 years instead of 5 years for the surface temperature response. Overall, the selection of number of years at the end of the simulations seem to weakly influence the efficacy results.

ERF was introduced to make it a good indicator of surface temperature change from various climate drivers ([Boucher et al., 2013](#); [Myhre et al., 2013](#); [Sherwood et al., 2015](#); [Forster et al., 2021](#)), in practice that is to have the efficacy of unity for all climate drivers. In the past several studies have shown that efficacy is unity in abrupt multi-model studies ([Richardson et al., 2019](#)) and in a comprehensive single-model study ([Hansen et al., 2005](#)). Here, we demonstrate that ERF is a good climate metric as multi-model simulations have efficacy close to unity in several realistic transient simulations. Our results show large model spread for aerosols, but unlike other studies no systematic differences from GHG experiments ([Shindell, 2014](#); [Salvi et al., 2022](#)).

## Data availability statement

CMIP6 model data used in this study are freely available from the CMIP6 repository on the Earth System Grid Federation nodes (<https://esgf-node.llnl.gov/search/cmip6/>, World Climate Research Programme, 2020). The PDRMIP data are available through the World Data Center for Climate (WDCC) <https://www.dkrz.de/up/systems/wdcc> with [https://doi.org/10.26050/WDCC/PDRMIP\\_2012-2021](https://doi.org/10.26050/WDCC/PDRMIP_2012-2021).

## Author contributions

GM: Conceptualization, Formal analysis, Investigation, Methodology, Visualization, Writing—original draft, Writing—review & editing. RB: Methodology, Writing—original draft, Writing—review & editing. TA: Methodology, Validation, Writing—original draft, Writing—review & editing. PF: Methodology, Validation, Writing—original draft, Writing—review & editing. CS: Methodology, Validation, Writing—original draft, Writing—review & editing.

## Funding

The author(s) declare that financial support was received for the research, authorship, and/or publication of this article. This study was supported by the European Union's Horizon 2020 research and innovation program under grant agreement no 820829 (CONSTRAIN project) and supported by the KeyCLIM project grant no. 295046 funded by the Norwegian Research Council. For PDRMIP parts of the computations were performed on and data has been interchanged shared and stored on resources provided by Sigma2 -the National Infrastructure for High-Performance Computing and Data Storage in Norway (project accounts NN9188K and NS9042K).

## Conflict of interest

The authors declare that the research was conducted in the absence of any commercial or financial relationships that could be construed as a potential conflict of interest.

The author(s) declared that they were an editorial board member of Frontiers, at the time of submission. This had no impact on the peer review process and the final decision.

## Publisher's note

All claims expressed in this article are solely those of the authors and do not necessarily represent those of their affiliated organizations, or those of the publisher,

the editors and the reviewers. Any product that may be evaluated in this article, or claim that may be made by its manufacturer, is not guaranteed or endorsed by the publisher.

## Supplementary material

The Supplementary Material for this article can be found online at: <https://www.frontiersin.org/articles/10.3389/fclim.2024.1397358/full#supplementary-material>

## References

- Andrews, T., Gregory, J. M., and Webb, M. J. (2015). The dependence of radiative forcing and feedback on evolving patterns of surface temperature change in climate models. *J. Clim.* 28, 1630–1648. doi: 10.1175/JCLI-D-14-00545.1
- Andrews, T., Smith, C. J., Myhre, G., Forster, P. M., Chadwick, R., and Ackerley, D. (2021). Effective radiative forcing in a GCM with fixed surface temperatures. *J. Geophys. Res.: Atmosph.* 126:e2020JD033880. doi: 10.1029/2020JD033880
- Boucher, O., Randall, D., Artaxo, P., Bretherton, C., Feingold, G., Forster, P., et al. (2013). "Clouds and Aerosols," in *Climate Change 2013: The Physical Science Basis. Contribution of Working Group I to the Fifth Assessment Report of the Intergovernmental Panel on Climate Change*, eds. T. F. Stocker, D. Qin, G.-K. Plattner, M. Tignor, S. K. Allen, J. Boschung, et al. (Cambridge, United Kingdom and New York, NY: Cambridge University Press), 571–657. doi: 10.1017/CBO9781107415324.016
- Cepi, P., and Gregory, J. M. (2019). A refined model for the Earth's global energy balance. *Climate Dynam.* 53, 4781–4797. doi: 10.1007/s00382-019-04825-x
- Etminan, M., Myhre, G., Highwood, E. J., and Shine, K. P. (2016). Radiative forcing of carbon dioxide, methane, and nitrous oxide: a significant revision of the methane radiative forcing. *Geophys. Res. Lett.* 43, 12614–12623. doi: 10.1002/2016GL071930
- Eyring, V., Bony, S., Meehl, G. A., Senior, C. A., Stevens, B., Stouffer, R. J., et al. (2016). Overview of the Coupled Model Intercomparison Project Phase 6 (CMIP6) experimental design and organization. *Geosci. Model Dev.* 9, 1937–1958. doi: 10.5194/gmd-9-1937-2016
- Forster, P., Storelvmo, T., Armour, K., Collins, W., Dufresne, J.-L., Frame, D., et al. (2021). "The earth's energy budget, climate feedbacks, and climate sensitivity," in *Climate Change 2021: The Physical Science Basis. Contribution of Working Group I to the Sixth Assessment Report of the Intergovernmental Panel on Climate Change*, eds. V. Masson-Delmotte, P. Zhai, A. Pirani, S. L. Connors, C. Péan, S. Berger, et al. (Cambridge: Cambridge University Press).
- Gillett, N. P., Shioyama, H., Funke, B., Hegerl, G., Knutti, R., Matthes, K., et al. (2016). The Detection and Attribution Model Intercomparison Project (DAMIP v1.0) contribution to CMIP6. *Geosci. Model Dev.* 9, 3685–3697. doi: 10.5194/gmd-9-3685-2016
- Gregory, J. M., and Andrews, T. (2016). Variation in climate sensitivity and feedback parameters during the historical period. *Geophys. Res. Lett.* 43, 3911–3920. doi: 10.1002/2016GL068406
- Hansen, J., Sato, M., Ruedy, R., Nazarenko, L., Lacis, A., Schmidt, G. A., et al. (2005). Efficacy of climate forcings. *J. Geophys. Res.-Atmosph.* 110:D18104. doi: 10.1029/2005JD005776
- Haugstad, A. D., Armour, K. C., Battisti, D. S., and Rose, B. E. J. (2017). Relative roles of surface temperature and climate forcing patterns in the inconstancy of radiative feedbacks. *Geophys. Res. Lett.* 44, 7455–7463. doi: 10.1002/2017GL074372
- Marvel, K., Schmidt, G. A., Miller, R. L., and Nazarenko, L. S. (2016). Implications for climate sensitivity from the response to individual forcings. *Nat. Clim. Chang.* 6, 386–389. doi: 10.1038/nclimate2888
- Modak, A., Bala, G., Caldeira, K., and Cao, L. (2018). Does shortwave absorption by methane influence its effectiveness? *Climate Dynam.* 51, 3653–3672. doi: 10.1007/s00382-018-4102-x
- Myhre, G., Forster, P. M., Samsel, B. H., Hodnebrog, Ø., Sillmann, J., Aalberg, S. G., et al. (2017). PDRMIP: a precipitation driver and response model intercomparison project—protocol and preliminary results. *Bull. Am. Meteorol. Soc.* 98, 1185–1198. doi: 10.1175/BAMS-D-16-0019.1
- Myhre, G., Shindell, D., Bréon, F.-M., Collins, W., Fuglestedt, J., Huang, J., et al. (2013). "Anthropogenic and natural radiative forcing," in *Climate Change 2013: The Physical Science Basis. Contribution of Working Group I to the Fifth Assessment Report of the Intergovernmental Panel on Climate Change*, eds. T. F. Stocker, D. Qin, G.-K. Plattner, M. Tignor, S.K. Allen, J. Boschung, et al. (Cambridge, United Kingdom and New York, NY: Cambridge University Press), 659–740. doi: 10.1017/CBO9781107415324.018
- Myhre, G., Stordal, F., Gausemel, I., Nielsen, C. J., and Mahieu, E. (2006). Line-by-line calculations of thermal infrared radiation representative for global condition: CFC-12 as an example. *J. Quant. Spectrosc. Radiat. Transf.* 97, 317–331. doi: 10.1016/j.jqsrt.2005.04.015
- Pincus, R., Forster, P. M., and Stevens, B. (2016). The Radiative Forcing Model Intercomparison Project (RFMIP): experimental protocol for CMIP6. *Geosci. Model Dev.* 9, 3447–3460. doi: 10.5194/gmd-9-3447-2016
- Previdi, M., Smith, K. L., and Polvani, L. M. (2021). Arctic amplification of climate change: a review of underlying mechanisms. *Environm. Res. Lett.* 16:093003. doi: 10.1088/1748-9326/ac1c29
- Quaas, J., Jia, H., Smith, C., Albright, A. L., Aas, W., Bellouin, N., et al. (2022). Robust evidence for reversal of the trend in aerosol effective climate forcing. *Atmos. Chem. Phys.* 22, 12221–12239. doi: 10.5194/acp-22-12221-2022
- Rantanen, M., Karpechko, A. Y., Lipponen, A., Nordling, K., Hyvärinen, O., Ruosteenoja, K., et al. (2022). The Arctic has warmed nearly four times faster than the globe since 1979. *Commun. Earth Environm.* 3:168. doi: 10.1038/s43247-022-00498-3
- Richardson, T. B., Forster, P. M., Smith, C. J., Maycock, A. C., Wood, T., Andrews, T., et al. (2019). Efficacy of climate forcings in PDRMIP models. *J. Geophys. Res.: Atmosph.* 124, 12824–12844. doi: 10.1029/2019JD030581
- Rugenstein, M., Bloch-Johnson, J., Gregory, J., Andrews, T., Mauritsen, T., Li, C., et al. (2020). Equilibrium climate sensitivity estimated by equilibrating climate models. *Geophys. Res. Lett.* 47:e2019GL083898. doi: 10.1029/2019GL083898
- Rugenstein, M. A., Caldeira, K., and Knutti, R. (2016). Dependence of global radiative feedbacks on evolving patterns of surface heat fluxes. *Geophys. Res. Lett.* 43, 9877–9885. doi: 10.1002/2016GL070907
- Salvi, P., Cepi, P., and Gregory, J. M. (2022). Interpreting differences in radiative feedbacks from aerosols versus greenhouse gases. *Geophys. Res. Lett.* 49:e2022GL097766. doi: 10.1029/2022GL097766
- Sherwood, S. C., Bony, S., Boucher, O., Bretherton, C., Forster, P. M., Gregory, J. M., et al. (2015). Adjustments in the forcing-feedback framework for understanding climate change. *Bull. Am. Meteorol. Soc.* 96, 217–228. doi: 10.1175/BAMS-D-13-00167.1
- Shindell, D. T. (2014). Inhomogeneous forcing and transient climate sensitivity. *Nat. Clim. Chang.* 4, 274–277. doi: 10.1038/nclimate2136
- Shindell, D. T., Faluvegi, G., Rotstayn, L., and Milly, G. (2015). Spatial patterns of radiative forcing and surface temperature response. *J. Geophys. Res.-Atmosph.* 120, 5385–5403. doi: 10.1002/2014JD022752
- Shine, K. P., Cook, J., Highwood, E. J., and Joshi, M. M. (2003). An alternative to radiative forcing for estimating the relative importance of climate change mechanisms. *Geophys. Res. Lett.* 30, 2047. doi: 10.1029/2003GL018141
- Smith, C. J., and Forster, P. M. (2021). Suppressed late-20th century warming in CMIP6 models explained by forcing and feedbacks. *Geophys. Res. Lett.* 48:e2021GL094948. doi: 10.1029/2021GL094948
- Smith, C. J., Harris, G. R., Palmer, M. D., Bellouin, N., Collins, W., Myhre, G., et al. (2021). Energy budget constraints on the time history of aerosol forcing and climate sensitivity. *J. Geophys. Res.: Atmosph.* 126:e2020JD033622. doi: 10.1029/2020JD033622

Smith, C. J., Kramer, R. J., Myhre, G., Alterskjær, K., Collins, W., Sima, A., et al. (2020). Effective radiative forcing and adjustments in CMIP6 models. *Atmos. Chem. Phys.* 20, 9591–9618. doi: 10.5194/acp-20-9591-2020

Zelinka, M. D., Myers, T. A., McCoy, D. T., Po-Chedley, S., Caldwell, P. M., Ceppi, P., et al. (2020). Causes of higher climate sensitivity in CMIP6 models. *Geophys. Res. Lett.* 47:e2019GL085782. doi: 10.1029/2019GL085782

Zhang, B., Zhao, M., He, H., Soden, B. J., Tan, Z., Xiang, B., et al. (2023). The dependence of climate sensitivity on the meridional distribution of radiative forcing. *Geophys. Res. Lett.* 50:e2023GL105492. doi: 10.1029/2023GL105492

Zhou, C., Wang, M., Zelinka, M. D., Liu, Y., Dong, Y., and Armour, K. C. (2023). Explaining forcing efficacy with pattern effect and state dependence. *Geophys. Res. Lett.* 50:e2022GL101700. doi: 10.1029/2022GL101700